Linearity Analysis of SiGe HBT Amplifiers Using a Power-Dependent Coefficient Volterra Technique

Junxiong Deng, Prasad S. Gudem, Lawrence E. Larson

Electrical and Computer Department, University of California San Diego, La Jolla, CA 92093

***Abstract* — To design high efficiency linear power amplifiers, it is always desired to clarify the main nonlinearity contributors in power amplifiers. The linearity of a silicon germanium (SiGe) heterojunction bipolar transistor (HBT) power amplifier is analyzed with the help of a power-dependent coefficient Volterra technique. The effect of emitter inductance is included and the dominant sources of nonlinearity are identified.**

***Index Terms* — Heterojunction bipolar transistors, intermodulation distortion, linearity, power amplifiers, Volterra series**

I. Introduction

The rapid development of third-generation wireless communication systems demands efficient modulation and multiple access schemes, such as Wide-band Code Division Multiple Access (WCDMA) [1]. Since these systems provide for improved network performance, more stringent linearity is required for the transmitter power amplifiers. At the same time, a high power-added-efficiency power amplifier is desirable for longer battery life. To design high efficiency linear power amplifiers, it is necessary to clarify the main nonlinearity contributors [2].

The linearity of RF amplifiers is usually analyzed using Volterra series. Besides providing insights into the nonlinearity mechanism, Volterra series can handle memory elements typical in the high power amplifier [3]-[6]. To keep the analysis tractable and preserve its accuracy, Volterra series is often truncated to third-order to analyze weakly nonlinear RF amplifiers operating in class-A mode [4]-[5]. On the other hand, high efficiency CDMA power amplifiers typically operate in the class-AB mode and exhibit strong nonlinearities. This renders the traditional Volterra analysis, truncated to third-order, inadequate and necessitates the inclusion of higher order terms, vastly increasing the complexity of the Volterra analysis. To keep the analysis tractable, and accurately predict the intermodulation distortion, we use a power-dependent coefficient Volterra technique [6]. Our analysis includes the effect of emitter bond-wire inductance, which is crucial to accurately predict the intermodulation distortion of power amplifiers. With the help of the power-dependent coefficient Volterra technique, the dominant sources of nonlinearity in SiGe heterojunction bipolar transistor (HBT) power amplifiers are highlighted.

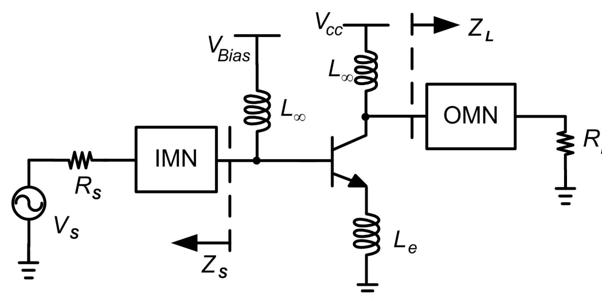

Fig. 1. Simplified schematic of a typical SiGe HBT power amplifier.

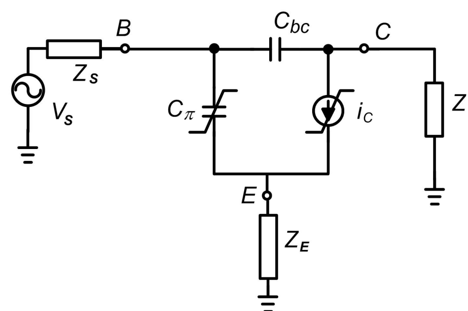

Fig. 2. Equivalent HBT nonlinear circuit for Volterra series calculation.

A power-dependent coefficient Volterra analysis technique is introduced in Section II. Experimental results are presented in Section III. The conclusions are summarized in Section IV.

II. Large-signal Nonlinear Analysis

A simplified schematic of a typical SiGe HBT power amplifier is shown in Fig. 1, and its equivalent nonlinear circuit for Volterra series calculation is shown in Fig. 2, where Z_S represents the source impedance, including the effects of the input matching network, bias network and base resistance of transistors; Z_L represents the load impedance, including the effects of the output matching

0-7803-8451-2/04/$20.00 ©2004 IEEE

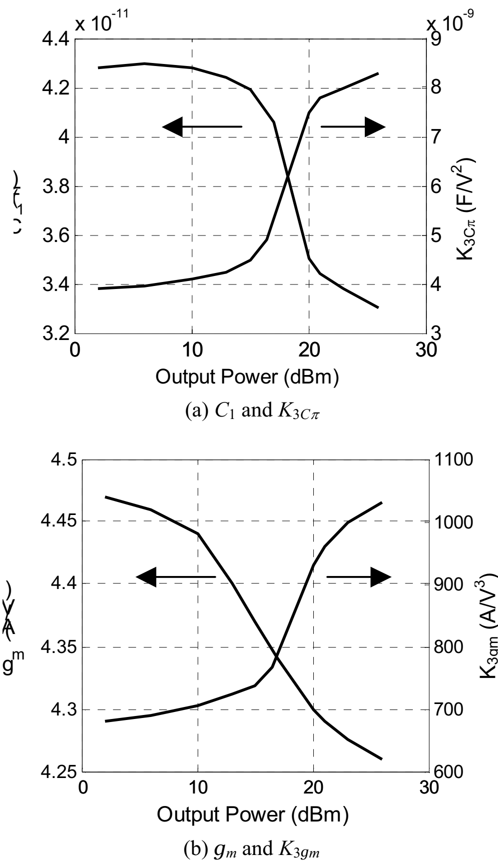

(a) C_1 and $K_{3C\pi}$

(b) g_m and K_{3gm}

Fig. 3. Simulated nonlinearity coefficients (a) C_1 and $K_{3C\pi}$, and (b) g_m and K_{3gm} versus output power, I_{CQ} = 110 mA.

network and output capacitance of transistors; Z_E represents the emitter impedance, including the bond-wire inductance and the ballasting resistance.

In our analysis, C_π and i_C are the main sources of nonlinearity and the remaining elements are assumed linear. Our simulations show that this is an adequate model to predict the nonlinearities in our power amplifier. Note that the nonlinear elements depend on both quiescent bias point and RF signal power. Therefore, their values have to be determined under large-signal conditions.

For the case of C_π, the stored charge in the base can be expressed as:

$$Q_\pi = C_1 v_{be} + K_{2C_\pi} v_{be}^2 + K_{3C_\pi} v_{be}^3 \qquad (1)$$

The RF input signal determines the excursion range of the base-emitter voltage, and this together with the quiescent bias condition determines the coefficients C_1, $K_{2C\pi}$ and $K_{3C\pi}$. The effects of the base-collector capacitance C_{bc} and the base resistance r_b are removed in calculating these coefficients.

Similarly, the nonlinear collector current i_C can be expressed as:

$$i_C = g_m v_{be} + K_{2g_m} v_{be}^2 + K_{3g_m} v_{be}^3 \qquad (2)$$

where g_m, K_{2gm} and K_{3gm} can be determined from the excursion of the base-emitter voltage together with the quiescent bias condition. The effects of capacitances and collector voltage variation are removed in calculating these coefficients.

The resulting nonlinearity coefficients C_1, $K_{3C\pi}$, g_m, and K_{3gm} are plotted in Fig. 3 for output power ranging from 0dBm to +26dBm. As shown in Fig. 4, $Z_S = 0$ at even-order harmonic frequencies (including $\omega_1 - \omega_2$ and $2\omega_1$) is achieved through use of a quarter-wave stub. With this additional simplification, the nonlinear transfer function can be derived using the method of nonlinear currents described in [7]-[8] by combining (1) and (2). With the assumption, $\omega_1 \cong \omega_2$ and $\omega_1, \omega_2 >> \omega_1 - \omega_2$, the third-order intermodulation ratio can be expressed as:

$$\begin{aligned} IMR_3 &= \frac{v_C(2\omega_1-\omega_2)}{v_C(\omega_1)} \\ &\cong \frac{3}{4} A_{vbe}^2(\omega_1) A_{vbe}(-\omega_2) \\ &\quad \{ K_{3C_\pi} [j\omega_1 Z_E + j\omega_1 Z_S + \omega_1^2 C_{bc} Z_S / g_m] \\ &\quad - K_{3g_m} / g_m [1 + j\omega_1 C_1 Z_E + j\omega_1 (C_1 + C_{bc}) Z_S] \} \cdot v_S^2 \end{aligned} \qquad (3)$$

where $A_{vbe}(\omega_1)$ and $A_{vbe}(-\omega_2)$ are the matching network voltage gains from the source to the base-emitter at frequencies ω_1 and $-\omega_2$ respectively, i.e.,

$$A_{Vbe}(\omega_1) = \frac{v_{be,\omega_1}}{v_S} = \frac{1 + j\omega_1 C_{bc} Z_L}{\det(\omega_1)} \qquad (4)$$

$$A_{Vbe}(-\omega_2) = \frac{v_{be,-\omega_2}}{v_S} = \frac{1 - j\omega_2 C_{bc} Z_L^*}{\det^*(\omega_2)} \qquad (5)$$

where,

$$\begin{aligned} \det(\omega_1) = 1 - \omega_1^2 (C_1 C_{bc} Z_E Z_L + C_1 C_{bc} Z_E Z_S + C_1 C_{bc} Z_L Z_S) \\ + g_m Z_E + j\omega_1 [C_1 Z_E + C_{bc} Z_L + C_1 Z_S + C_{bc} Z_S \\ + C_{bc} g_m Z_E Z_L + C_{bc} g_m Z_E Z_S + C_{bc} g_m Z_L Z_S] \end{aligned} \qquad (6)$$

III. Experimental Results

The single-stage power amplifier shown in Fig. 4 was fabricated in a 0.25 μm SiGe BiCMOS process [9]. The main bipolar transistors in the power amplifier are composed of 100 devices, each with an emitter area of 48 μm 0.44 μm. The devices were packaged in the Amkor Micro-Lead-Frame (MLF) package. The chip was mounted on a Rogers20 PCB board. The quiescent bias current at the collector is 110 mA.

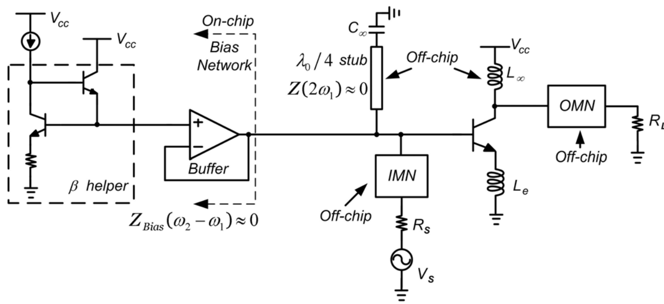

Fig. 4. Schematic of circuit used for experimental verification of linearity analysis.

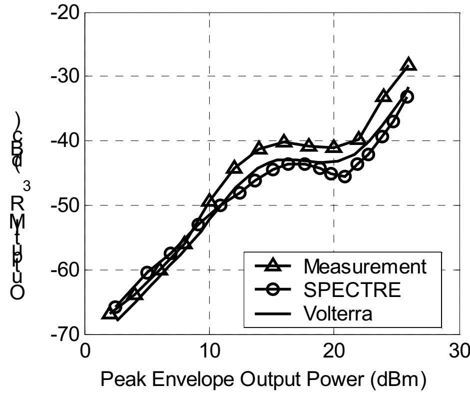

Fig. 5. IMR_3 comparison between SPECTRE simulation, Volterra calculation, and measurement for the circuit of Fig. 4.

A comparison of IMR_3 obtained from experimental measurements with our Volterra expression in (3) shows good agreement throughout the entire range of output powers from 0 dBm to +26 dBm (Fig. 5). In addition, the excellent agreement of IMR_3 between SPECTRE simulations and our Volterra expression validates the completeness of our model shown in Fig. 2 and the corresponding extraction methodology described in the section II.

Our analysis not only accurately predicts the IMR_3, but also provides insight into the individual contributions from the main nonlinear sources. Fig. 6 displays the calculated amplitude and phase of IMR_3 in three cases:

1) with the effect of the nonlinearity of C_π only (K_{3g_m}=0);
2) with the effect of the nonlinearity of i_C only ($K_{3C\pi}$=0);
3) with the effects of the nonlinearities of C_π and i_C together.

We observed that the nonlinearity of C_π and the nonlinearity of i_C are quite large over the whole power range, but they are opposite in phase, resulting in the well-known intermodulation cancellation effect [10]. At low input powers the nonlinearity of i_C dominates the magnitude and the phase of output IMR_3. The C_π nonlinearity dominates at high input powers so that the output IMR_3 is determined by the C_π nonlinearity. The overall linearity of the SiGe HBT PA depends on the degree to which this cancellation is achieved [11].

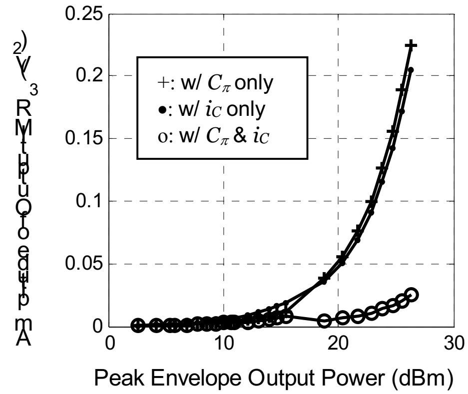

(a) amplitude of IMR_3

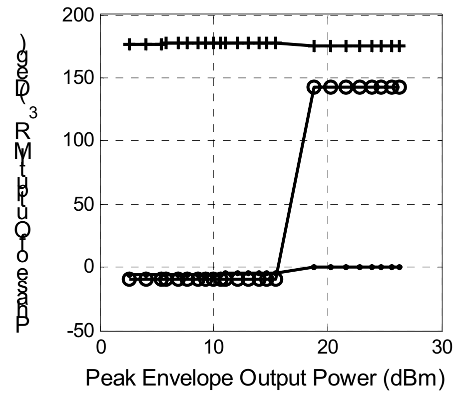

(b) phase of IMR_3

Fig. 6. Individual contributions to amplitude and phase of output IMR_3. Note that the jump in the phase of output IMR_3 comes from the fact that: at low input powers the nonlinearity of i_C dominates the phase of output IMR_3, whereas at high input powers the C_π nonlinearity dominates the phase of output IMR_3.

Furthermore, the linearity is analyzed with different emitter bond-wire inductance (L_e) in Fig. 7. Fig. 8 and Fig. 9 show how power gain and efficiency change with L_e. For our power amplifier, we found that 80 pH is the optimum value for bond-wire inductance L_e, considering the tradeoff between gain, linearity and efficiency.

IV. Conclusions

This paper used a power-dependent coefficient Volterra technique to analyze the linearity of SiGe HBT power amplifiers. The analyzed model takes into account the effect of emitter bond-wire inductance. The comparison of IMR_3 between analysis, simulation and measurement data has validated this approach. The main sources of

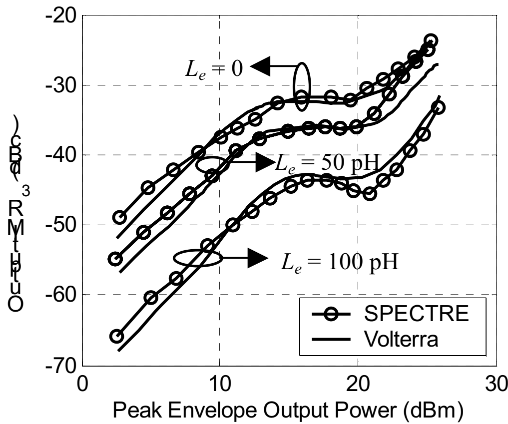

Fig. 7. IMR_3 with different values of L_e, I_{CQ} = 110 mA.

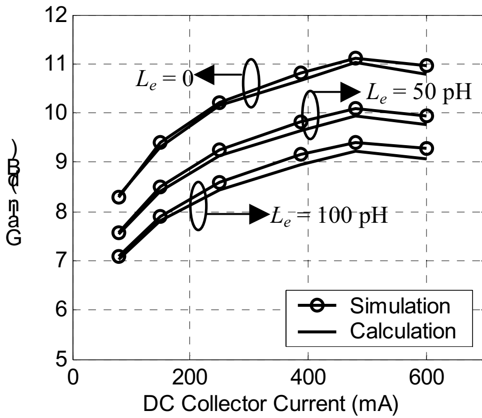

Fig. 8. Comparison of simulated and calculated power gains with different values of L_e.

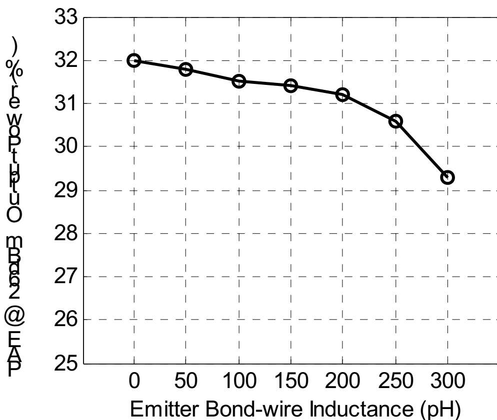

Fig. 9. Simulated power added efficiencies at 26 dBm output power with different values of L_e.

nonlinearity in SiGe HBT power amplifiers are highlighted.

ACKNOWLEDGEMENT

The authors would like to acknowledge the continuous support of the Center of Wireless Communications at University of California, San Diego, and its member companies and a University of California Discovery Grant, as well as the invaluable discussion with Dr. Chengzhou Wang, Dr. Mani Vaidyanathan, Mr. Horace Ng and Ms. Annie Yang.

REFERENCES

[1] W. Lu, "Third-generation wireless mobile communications and beyond", *Personal Communications, IEEE [see also IEEE Wireless Communications]*, Vol. 7, pp. 5, Dec. 2000.

[2] J. Vuolevi, T. Rahkonen, *Distortion in RF Power Amplifiers*, Artech House, 2003.

[3] J. Vuolevi and T. Rahkonen, "Analysis of third-order intermodulation distortion in common-emitter BJT and HBT amplifiers," *Circuits and Systems II, IEEE Transactions on*, vol. 50, pp994–1001, Dec 2003.

[4] R.A. Minasian, "Intermodulation Distortion Analysis of MESFET Amplifiers Using the Volterra Series Representation," *Microwave Theory and Techniques, IEEE Transactions on*, vol. 28, pp.1–8, Jan 1980.

[5] A.E. Parker and G. Qu, "Intermodulation nulling in HEMT common source amplifiers," *Microwave and Wireless Components Letters, IEEE*, vol. 11, pp.109–111, March 2001.

[6] C. Wang, M. Vaidyanathan, and L.E. Larson, "A Capacitance-Compensation Technique for Improved Linearity in CMOS Class-AB Power Amplifiers," *IEEE Journal of Solid-State Circuits*, to be published.

[7] S.A. Maas, *Nonlinear Microwave Circuits*, Norwood, MA: Artech House, 1988.

[8] P. Wambacq, W. Sansen, *Distortion Analysis of Analog Integrated Circuits*, KAP, 1998.

[9] IBM 6HP BiCMOS process, http://www-3.ibm.com/chips/techlib/techlib.nsf/products/BiCMOS_6HP.

[10] S.A. Maas, B.L. Nelson, and D.L. Tait, "Intermodulation in heterojunction bipolar transistors," *Microwave Theory and Techniques, IEEE Transactions on*, vol. 40, pp.442–448, March 1992.

[11] M. Vaidyanathan, M. Iwamoto, L.E. Larson, P.S. Gudem, and P.M. Asbeck, "A theory of high-frequency distortion in bipolar transistors," *Microwave Theory and Techniques, IEEE Transactions on*, vol. 51, pp.448–461, Feb 2003.